

Control over Photoinduced Energy and Electron Transfer in Supramolecular Polyads of Covalently linked azaBODIPY-Bisporphyrin 'Molecular Clip' Hosting Fullerene

Francis D'Souza,^{*,†,‡} Anu N. Amin,[‡] Mohamed E. El-Khouly,[§] Navaneetha K. Subbaiyan,[†] Melvin E. Zandler,[‡] and Shunichi Fukuzumi^{*,§,||}

[†]Department of Chemistry, University of North Texas, 1155 Union Circle, #305070, Denton, Texas 76203-5017, United States

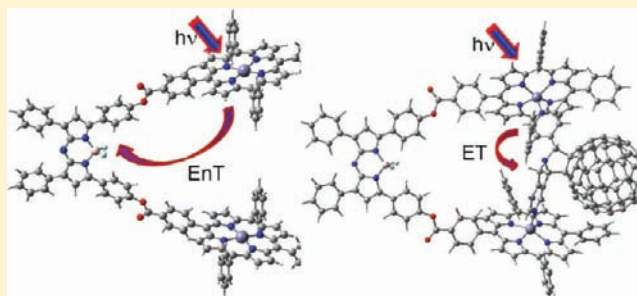
[‡]Department of Chemistry, Wichita State University, 1845, Fairmount, Wichita, Kansas 67260-0051, United States

[§]Graduate School of Engineering, Osaka University, ALCA, Japan Science and Technology Agency (JST), Suita, Osaka 565-0871, Japan

^{||}Department of Bioinspired Science, Ewha Woman's University, Seoul, 120-750, Korea

S Supporting Information

ABSTRACT: A 'molecular clip' featuring a near-IR emitting fluorophore, BF₂-chelated tetraarylazadipyromethane (aza-BODIPY) covalently linked to two porphyrins (MP, M = 2H or Zn) has been newly synthesized to host a three-dimensional electron acceptor fullerene via a 'two-point' metal–ligand axial coordination. Efficient singlet–singlet excitation transfer from ¹ZnP* to aza-BODIPY was witnessed in the dyad and triad in nonpolar and less polar solvents, such as toluene and *o*-dichlorobenzene, however, in polar solvents, additional electron transfer occurred along with energy transfer. A supramolecular tetrad was formed by assembling bis-pyridine functionalized fullerene via a 'two-point' metal–ligand axial coordination, and the resulted complex was characterized by optical absorption and emission, computational, and electrochemical methods. Electron transfer from photoexcited zinc porphyrin to C₆₀ is witnessed in the supramolecular tetrad from the femtosecond transient absorption spectral studies. Further, the supramolecular polyads (triad or tetrad) were utilized to build photoelectrochemical cells to check their ability to convert light into electricity by fabricating FTO/SnO₂/polyad electrodes. The presence of azaBODIPY and fullerene entities of the tetrad improved the overall light energy conversion efficiency. An incident photon-to-current conversion efficiency of up to 17% has been achieved for the tetrad modified electrode.



■ INTRODUCTION

Biomimetic artificial photosynthetic systems aimed at solar energy conversion and fuel production must integrate modular molecular entities to collect and funnel light energy, generate charge-separated species, and transport the generated chemical energy to the catalytic sites for water oxidation and CO₂ reduction, similar to the natural photosynthetic systems.¹ Over the years, extensive efforts have been devoted to tackle every facet of this complex problem by molecularly engineering the supramolecular systems; however, components that are both efficient and robust and integrated into one working system remain a major challenge.^{2–7} Novel design of light-funneling, photoconversion, and catalytic modules capable of self-ordering and self-assembling into an integrated functional unit will make an efficient artificial photosynthetic system possible.^{8,9}

The three-dimensional electron acceptors, fullerenes, have stimulated interest due to their extraordinary electron acceptor properties that was predicted theoretically and confirmed

experimentally.^{10–14} Supramolecular systems involving a variety of electron donors (such as porphyrin, phthalocyanine, etc.) and fullerene have made considerable advances in the areas of light-induced electron-transfer chemistry and light energy harvesting.^{2–9,15–19} These breakthroughs are mainly due to the small reorganization energy of fullerenes in electron-transfer reactions¹¹ that would lead to ultrarapid charge separation together with slow charge recombination leading unprecedentedly long-lived charge-separated states with high quantum efficiencies.^{12,20} Additionally, such studies have shed light on fundamental understanding of electron-transfer aspects, such as distance and orientation factors related to supramolecular organization, electronic coupling elements, reorganization energies, electron tunneling, etc.^{3–9,15–20}

Recently, a structural analog of a well-known fluorophore, BF₂-chelated dipyrromethane (BODIPY or BDP),²¹ namely,

Received: October 16, 2011

Published: November 24, 2011

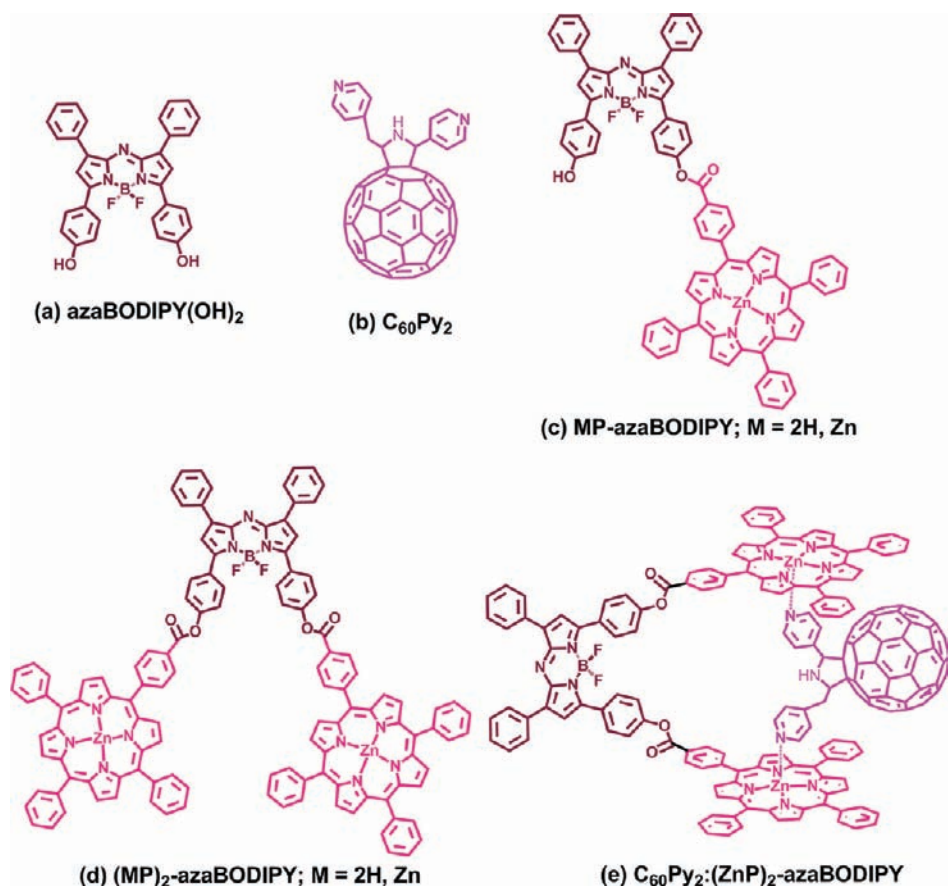


Figure 1. Structure of (a) aza(BODIPY(OH))₂, (b) bispyridine functionalized fullerene, C₆₀Py₂, (c) MP-azaBODIPY (M = 2H or Zn) dyads, (d) (MP)₂-azaBODIPY (M = 2H or Zn) triads, and (e) supramolecular tetrad, C₆₀Py₂:(ZnP)₂-azaBODIPY investigated in the present study.

BF₂-chelated tetraarylazadipyromethanes (azaBODIPY or ADP), with a nitrogen in the meso position of the macrocycle has attracted increasing attention, because of their high extinction coefficients ($7\text{--}8 \times 10^5 \text{ M}^{-1} \text{ cm}^{-1}$) and large fluorescence quantum yields beyond 700 nm.^{22,23} Thus, they have been used in applications ranging from sensors and photodynamic therapy agents.^{24,25} Importantly, as needed for electron-transfer applications, the azaBODIPYs are considerably easier to reduce compared to BODIPY and exhibit diagnostic spectral bands of the one-electron reduced products in the near-IR region, sufficiently far from the triplet absorption bands of the partnering donor/acceptor entities. Recently, we exploited this property of aza-BODIPY by synthesizing covalently linked donor–acceptor dyads and triads featuring azaBODIPY and ferrocene and demonstrated efficient photo-induced electron transfer (PET) from ferrocene to the singlet excited azaBODIPY using transient absorption techniques.²⁶ Further, by replacing the ferrocene entities by BODIPY entities, PET from the singlet excited BODIPY to azaBODIPY was successfully demonstrated.²⁷ The one-electron reduction potential of azaBODIPY is more positive by about 200 mV than that of C₆₀.²⁸ Thus, a combination of aza-BODIPY and C₆₀ as electron acceptors together with a well-known photosensitizer electron donor, zinc porphyrin, provides an outstanding opportunity to construct brilliant photosynthetic reaction center models, in which a wide range of visible light can be absorbed.

We report herein synthesis and photodynamics of supramolecular polyads of covalently linked azaBODIPY-bisporphyrin

in ‘molecular clip’ hosting fullerene, as shown in Figure 1e. The azaBODIPY is functionalized to have one and two porphyrin entities (Figure 1c and d). The two ZnP entities of the triad are spatially arranged in a ‘molecular clip’ structure to accommodate the bispyridine functionalized fullerene (Figure 1b) via a ‘two-point’ metal–ligand axial coordination to ultimately generate supramolecular tetrad, as shown in Figure 1e. In the absence of fullerene, photoinduced energy transfer from the singlet excited MP to azaBODIPY in the dyads and triads is expected to occur due to spectral matching and energetics. Switching of electronic processes has been realized in C₆₀py₂:(ZnP)₂-azaBODIPY supramolecular tetrad. Upon introducing fullerene spatially close to the electron donor, electron transfer leading to the charge-separated species is expected. That is, noncovalent assembly of building blocks to direct the formation of the photo/electroactive supramolecules exhibiting features that would otherwise be difficult to attain in a single molecule is envisioned. It should be noted that the behavior of the examined C₆₀py₂:(ZnP)₂-azaBODIPY supramolecular tetrad is quite different from the reported bis(phenylethynyl)-anthracene-BODIPY-ZnP:C₆₀py₂ heptad, which is acting as a classical antenna–reaction center complex.^{14b} Systematic photochemical studies have been performed to demonstrate the photoinduced intramolecular events of the examined compounds. Furthermore, the ability of the present supramolecular polyads (triad and tetrad) in direct conversion of light into electricity has been tested by constructing photoelectrochemical cells on FTO/SnO₂ modified surfaces. Improved photo-

current efficiencies in the case of tetra modified electrode as compared to the control triads are observed.

RESULTS AND DISCUSSION

Studies of MP-azaBODIPY Dyads and (MP)₂-azaBODIPY Triads. Syntheses of MP-azaBODIPY Dyads and (MP)₂-azaBODIPY Triads. The syntheses of the porphyrin-azaBODIPY systems involved a multistep approach, as detailed in the Experimental Section. Briefly, the BF₂ chelated [5-(4-hydroxyphenyl)-3-phenyl-1H-pyrrol-2-yl]-[5-(4-hydroxyphenyl)-3-phenylpyrrol-2-ylidene]amine was synthesized according to our earlier reported procedure.²⁶ Next, this compound was treated with 5-(4'-carboxyphenyl)-10,15,20-triphenylporphyrin in the presence of EDCI to introduce one or two free-base porphyrin entities on the azaBODIPY periphery. The free-base porphyrins were subsequently metalated to obtain the respective ZnP-azaBODIPY dyad and the (ZnP)₂-azaBODIPY triad. The structural integrity of the newly synthesized compounds was established from ¹H NMR, mass (see Figure S1, Supporting Information) and other optical techniques.

Steady-State Absorption and Fluorescence Measurements. Figure 2a shows the normalized (to the Soret band

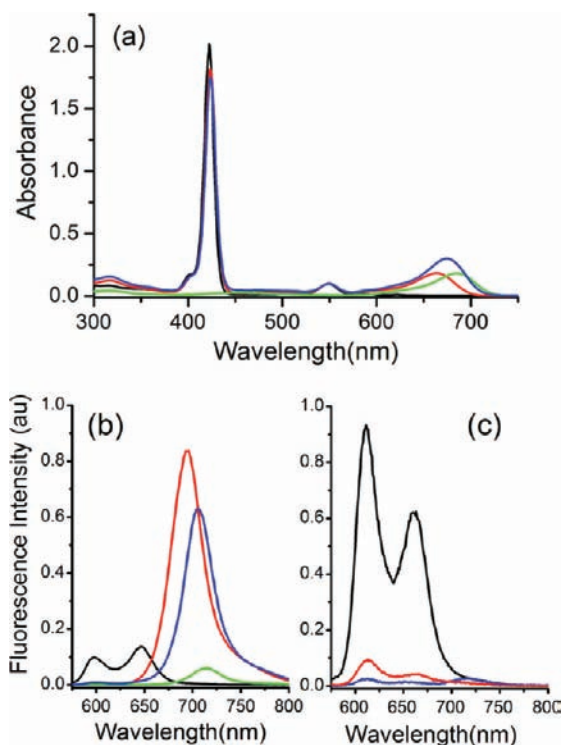


Figure 2. (a) Normalized (to the Soret band) absorption spectra in toluene, (b) emission spectra in toluene ($\lambda_{\text{ex}} = 549 \text{ nm}$), and (c) emission spectra in benzonitrile ($\lambda_{\text{ex}} = 560 \text{ nm}$) of ZnP (black), azaBODIPY(OH)₂ (green), ZnP-azaBODIPY dyad (blue), and the (ZnP)₂-azaBODIPY triad (red) compounds.

of porphyrin) optical absorption spectra of the ZnP-azaBODIPY dyad and the (ZnP)₂-azaBODIPY triad along with the control compounds, viz., zinc tetraphenylporphyrin (ZnP) and azaBODIPY(OH)₂ in toluene. ZnP exhibited a strong Soret at 422 nm and visible bands at 550 and 587 nm. The azaBODIPY(OH)₂ control (Figure 1a) had a strong absorption at 685 nm and a weak band at 316 nm. The ZnP-

azaBODIPY dyad and the (ZnP)₂-azaBODIPY triad exhibited bands corresponding to both the entities.

However, for the triad, the azaBODIPY intensity was roughly half of that observed for dyad owing to the presence of two ZnP entities. It is interesting to note that the band position of the azaBODIPY depended upon the number of free hydroxyl groups on the macrocycle, that is, each -OH group caused about 10 nm bathochromic shifts. The spectral features of the free-base porphyrin derivatives were also similar (Figure S2a, Supporting Information). Changing the solvent to more polar benzonitrile also revealed such trends, however, with slightly larger bathochromic shifts (Figure S2b and S2c, Supporting Information).

Figure 2b shows the fluorescence emission spectra of the investigated compounds in nonpolar toluene. By the Q-band excitation of the control ZnP, two emission bands at 560 and 647 nm were observed. At this excitation wavelength, azaBODIPY(OH)₂ revealed a weak emission band at 714 nm due to direct excitation of the fluorophore. Interestingly, for the dyads and triad, the ZnP emission was found to be totally quenched with the appearance of new emission bands corresponding to azaBODIPY entity, suggestive of the occurrence of excitation transfer in the dyad and triad.²⁹ In a control experiment, the emission spectra of equimolar mixture of ZnP and azaBODIPY under similar experimental conditions were recorded. Such spectra revealed no quenching of ZnP (<5%) or enhanced emission of azaBODIPY, suggesting the observed energy transfer in the dyad and triad to be an intramolecular event. The excitation transfer for (ZnP)₂-azaBODIPY triad was found to be slightly higher than that of ZnP-azaBODIPY dyad perhaps due to the presence of two ZnP entities of the triad. In a slightly polar solvent, *o*-dichlorobenzene, a similar spectral trend was observed although the intensity of the energy-transfer product, azaBODIPY, emission was slightly lower (vide infra).

In order to confirm the occurrence of energy transfer in nonpolar solvents, the excitation spectra of the dyad and triad were recorded by holding the excitation monochromator to the emission maxima of azaBODIPY, and the results are shown in Figure S3 (Supporting Information). These spectra revealed peaks not only of azaBODIPY but also that of ZnP for the both the dyad and triad. Such features (ZnP peaks) were not observed for the spectrum recorded for the equimolar mixture of ZnP and azaBODIPY.

On the contrary, changing the solvent to polar benzonitrile revealed quenching of the MP emission with no emission corresponding to azaBODIPY, as shown in Figure 2c. Control ZnP emission in benzonitrile was located at 610 and 660 nm, while azaBODIPY(OH)₂ at this excitation wavelength revealed a band at 735 nm which is nearly 20 nm red-shifted from that observed in toluene. In the case of ZnP-azaBODIPY dyad and (ZnP)₂-azaBODIPY triad, the ZnP emission was quenched over 97 and 90%, respectively, with no emission of azaBODIPY indicating additional photochemical events in polar benzonitrile solvent.³⁰

The dyad and triad derived from the free-base porphyrin, H₂P-azaBODIPY, and the (H₂P)₂-azaBODIPY also revealed similar spectral features in spite of the red-shifted emission bands of H₂P compared to ZnP (Figure S4, Supporting Information). Thus, energy transfer in toluene and donor H₂P emission quenching perhaps due to additional electron transfer in benzonitrile were envisioned.

Computational Studies of the Dyad and Triad. Figure 3a and b shows the B3LYP/3-21G(*)^{31,32} optimized structures of

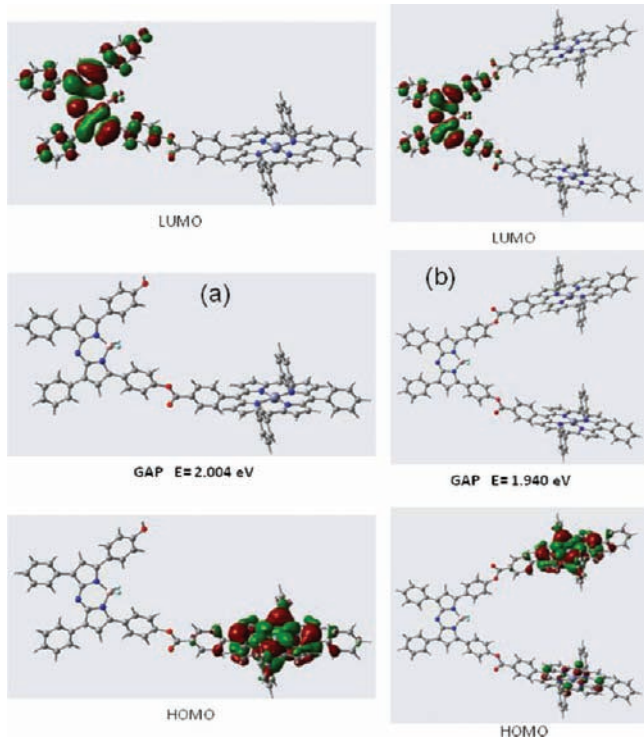


Figure 3. B3LYP/3-21G(*) optimized structure of (a) ZnP-azaBODIPY dyad and (b) the (ZnP)₂-azaBODIPY triad. In the top and bottom panels, each figure shows the frontier LUMO and HOMO of the respective molecule.

the ZnP-azaBODIPY dyad and (ZnP)₂-azaBODIPY triad, respectively. The structures are fully optimized on a Born–Oppenheimer potential energy surface. In the optimized structure of ZnP-azaBODIPY, both the azaBODIPY and ZnP macrocycles are found to be flat with a slight tilt of the peripheral aromatic rings of azaBODIPY. The boron–Zn distance was found to be 16.0 Å, while the distance between the closest carbon of BDP to the closest carbon of ADP (edge-to-edge distance) was ~12.08 Å. The two macrocycles were spatially disposed with a dihedral angle of 77°. Interestingly, for the (ZnP)₂-azaBODIPY triad, the two coplanarly positioned ZnP entities linked to azaBODIPY formed a molecular clip-type structure with a Zn–B–Zn angle of 60°. The two ZnP macrocycles are separated by a distance of 15.8 Å (Zn–Zn distance), while the B–Zn and edge-to-edge distances were found to be nearly the same for the two ZnP-azaBODIPY segments of the triad. For the dyad and triad, the highest occupied molecular orbital (HOMO) was on the ZnP entity, while the lowest unoccupied molecular orbital (LUMO) was on the azaBODIPY entity. The location of the HOMO and LUMO suggests the ZnP entity to be an electron donor and the azaBODIPY entity to be an electron acceptor.

Electrochemistry and Energy Levels of the Dyad and Triad. In order to establish the energy levels, electrochemical studies using differential pulse voltammetry (DPV) were performed. Figure 4 shows DPVs of the dyads and triads along with the control compounds in benzonitrile containing 0.10 M of (*n*-Bu₄N)ClO₄, while the redox data are summarized in Table 1. AzaBODIPY revealed both one electron reduction

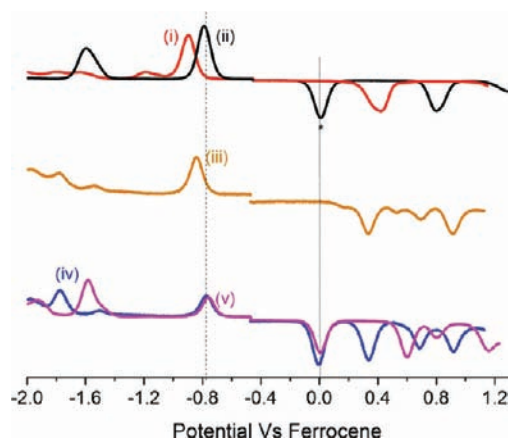


Figure 4. Differential pulse voltammograms of (i) azaBODIPY(OH)₂, (ii) azaBODIPY, (iii) ZnP-azaBODIPY, (iv) (ZnP)₂-azaBODIPY, and (v) (H₂P)₂-azaBODIPY in benzonitrile and 0.10 M of (*n*-Bu₄N)ClO₄. Scan rate = 5 mV/s, pulse width = 0.25 s, and pulse height = 0.025 V. The asterisk in the top panel shows oxidation process of ferrocene used as an internal standard.

Table 1. Electrochemical Redox Potentials (V vs Fc/Fc⁺), Energy Levels of the Charge-Separated States (ΔG_{CR}) and Free-Energy Changes for Charge Separation (ΔG_{CS}) for the MP-azaBODIPY (M = 2H or Zn) Dyads and Triads in Benzonitrile

compound	MP ^{0/+} /V	azaBODIPY ^{0/+} /V	$-\Delta G_{CR}^a$ /eV	$-\Delta G_{CS}^b$ /eV
azaBODIPY	–	–0.79	–	–
azaBODIPY(OH) ₂	–	–0.90	–	–
ZnP-azaBODIPY	0.33	–0.84	1.17	0.88
(ZnP) ₂ -azaBODIPY	0.33	–0.77	1.10	0.95
H ₂ P-azaBODIPY	0.60	–0.84	1.44	0.46
(H ₂ P) ₂ -azaBODIPY	0.60	–0.76	1.36	0.54

^a $\Delta G_{CR} = e(E_{ox} - E_{red})$. The electrostatic term was neglected due to the use of a polar solvent (PhCN). ^b $-\Delta G_{CS} = \Delta E_{0-0} - \Delta G_{CR}$, where ΔE_{0-0} is the energy of the lowest excited states of porphyrins being 2.05 eV for ZnP and 1.90 eV for H₂P.

and oxidation processes located at –0.79 and 0.80 V vs Fc/Fc⁺, respectively. The first reduction was found to be cathodically shifted by over 200 mV compared with the well-known electron acceptor, C₆₀.¹⁰ Introducing the hydroxyphenyl groups on azaBODIPY caused the reduction to be harder by about 100 mV, while the oxidation process was irreversible (from cyclic voltammetric experiments), however, with cathodically shifted potentials by nearly 380 mV.

For ZnP-azaBODIPY dyad and (ZnP)₂-azaBODIPY triad, the ZnP oxidation occurred at around 0.33 V vs Fc/Fc⁺, while the first reduction of the porphyrin entity occurred at –1.54 V vs Fc/Fc⁺. The azaBODIPY reduction in the dyad was located at –0.84, while for the triad, it was located at –0.77 V vs Fc/Fc⁺. In the case of free-base porphyrin derivatives, the first oxidation corresponding to H₂P was located at 0.60 V, while the first reduction was located at –1.50 V vs Fc/Fc⁺. The peak potentials of azaBODIPY tracked that of the ZnP-azaBODIPY analogs. These results collectively suggest both free-base and zinc(II) porphyrins being electron rich and azaBODIPY being electron deficient in these molecular systems. Since there were no appreciable changes in the oxidation potentials of the porphyrin entities when compared to the pristine porphyrin

derivatives in the dyads and triads, absence of inter- or intramolecular interactions was envisioned.

The energies of the charge-separated states were calculated using the redox, geometric, and optical data according to Weller's approach,³³ and the calculated values are given in Table 1. By comparing these energy levels of the charge-separated states with the energy levels of the excited states, the driving forces of charge separation (ΔG_{CS}) were also evaluated. The generation of MP^{*+} -azaBODIPY $^{*-}$ ($M = 2H$, or Zn) for the dyads and triads was found to be exergonic via the singlet excited state of MP in benzonitrile.

Femtosecond Transient Absorption Spectral Studies of $(MP)_n$ -azaBODIPY ($M = 2H$ or Zn , $n = 1, 2$). Femtosecond transient absorption spectroscopy was used to obtain further insight into the excited state events of $(ZnP)_n$ -azaBODIPY and $(H_2P)_n$ -azaBODIPY ($n = 1, 2$) dyads and triads to corroborate the proposed energy- and electron-transfer processes. Toward this end, $(ZnP)_n$ -azaBODIPY and $(H_2P)_n$ -azaBODIPY were probed with 426 nm excitation to selectively excite the porphyrin fluorophore. The femtosecond transient absorption spectra of the ZnP reference in toluene (Figure S6, Supporting Information) revealed the instantaneous formation of the $^1ZnP^*$ with a transient absorption maxima at 458 nm, which decayed slowly ($7.8 \times 10^8 \text{ s}^{-1}$) to populate the $^3ZnP^*$ with a maximum at 480 nm.

The spectral features in the visible region, which were seen immediately (i.e., 1 ps) upon excitation of ZnP -azaBODIPY in toluene (Figure 5), were almost the same as those recorded for

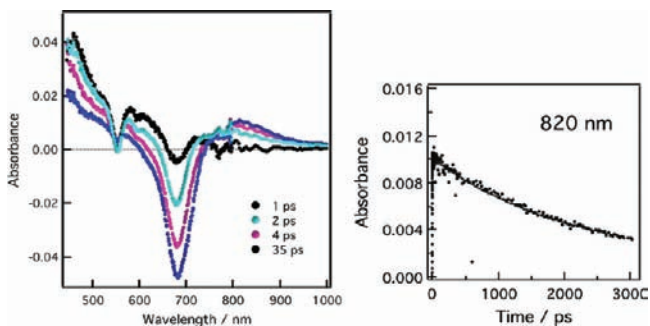


Figure 5. (Left) Differential absorption spectra obtained upon femtosecond flash photolysis (426 nm) of ZnP -azaBODIPY in toluene at the indicated time intervals. (Right) The decay profile of the formed singlet azaBODIPY at 820 nm.

the ZnP singlet excited state ($^1ZnP^*$). With time, the ZnP singlet emission peak at 458 nm diminished in intensity with concomitant increase of the azaBODIPY emission at 682 and 820 nm, providing direct evidence of excitation transfer between the $^1ZnP^*$ and azaBODIPY. The kinetics of $^1ZnP^*$ to azaBODIPY energy transfer was determined by exponential fitting of the rise profile of the formed $^1azaBODIPY^*$ at 820 nm ($k_{ENT} = 6.6 \times 10^{11} \text{ s}^{-1}$). Further, the decay rate of the formed $^1azaBODIPY^*$ was determined as $4.6 \times 10^8 \text{ s}^{-1}$, which is close to the decay of pristine $^1azaBODIPY^*$ indicating lack of quenching by the attached ZnP in toluene. Similar absorption spectra were observed in the case of $(ZnP)_2$ -azaBODIPY triad in deaerated toluene (Figure S7, Supporting Information). The k_{ENT} was found to be $1.0 \times 10^{12} \text{ s}^{-1}$, which was faster than that of ZnP -azaBODIPY dyad.

By changing the solvent from toluene to benzonitrile, the transient absorption spectra of the dyad and triad exhibited

diminished $^1ZnP^*$ emission at 458 nm with the concomitant increase of the $^1azaBODIPY^*$ emission at 682 and 820 nm, providing direct evidence of energy transfer in the polar media (Figure 6). From the decay profile of the $^1ZnP^*$ and the rise

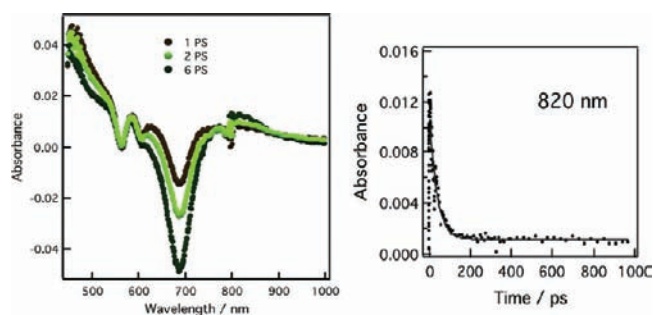


Figure 6. (Left) Differential absorption spectra obtained upon femtosecond flash photolysis (426 nm) of ZnP -azaBODIPY in benzonitrile at the indicated time intervals. (Right) The decay profile of the formed $^1azaBODIPY^*$ at 820 nm.

profile of the formed $^1azaBODIPY^*$, the $^1ZnP^*$ to azaBODIPY energy transfer in polar benzonitrile was determined to be $6.4 \times 10^{11} \text{ s}^{-1}$. Similar spectral observations were also made in the case $(ZnP)_2$ -azaBODIPY triad wherein the k_{ENT} was found to be $9.6 \times 10^{11} \text{ s}^{-1}$ (Figure S8a, Supporting Information), slightly faster than that observed for the dyad.

Interestingly, in polar benzonitrile, the energy-transfer product of the dyad and triad, $^1azaBODIPY^*$ revealed faster decay than that observed for pristine azaBODIPY indicating subsequent PET from ZnP to the $^1azaBODIPY^*$ to produce $(ZnP)_n^{*+}$ -azaBODIPY $^{*-}$ charge separation product, taking into account that the energy transfer from $^1azaBODIPY^*$ to ZnP is not feasible. Based on the decay rates of the control $^1azaBODIPY^*$ and the examined compounds, the k_{CS} measured for the dyad and triad was found to be 2.9×10^{10} and $4.5 \times 10^{10} \text{ s}^{-1}$, respectively. Similar observations were also made for the investigated H_2P -azaBODIPY dyad (Figure 7) and $(H_2P)_2$ -

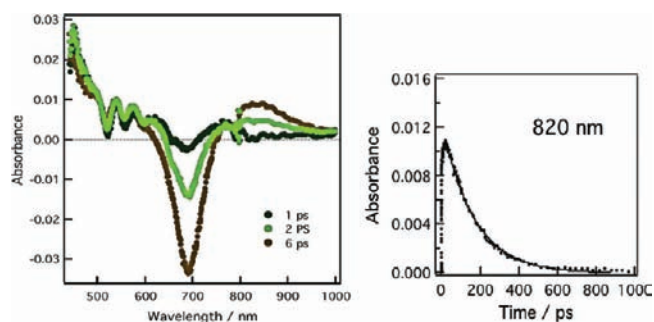


Figure 7. (Left) Differential absorption spectra obtained upon femtosecond flash photolysis (426 nm) of H_2P -azaBODIPY in benzonitrile at the indicated time intervals. (Right) The decay profile of the formed $^1azaBODIPY^*$ at 820 nm.

azaBODIPY triad (Figure S8b, Supporting Information), where energy transfer from $^1H_2P^*$ to azaBODIPY (k_{ENT}) followed by electron transfer from H_2P to $^1azaBODIPY^*$ (k_{CS}) was clearly observed. The k_{ENT} and k_{CS} measured for these processes were found to be 2.3×10^{11} and $6.0 \times 10^9 \text{ s}^{-1}$ for the H_2P -azaBODIPY dyad and 4.0×10^{11} and $1.6 \times 10^{10} \text{ s}^{-1}$ for the $(H_2P)_2$ -azaBODIPY triad, respectively.

The kinetic data for the photochemical processes of the investigated dyads and triads are summarized in Table 2. In

Table 2. Rates of Singlet–Singlet Energy Transfer from $^1\text{MP}^*$ to azaBODIPY (in Toluene and Benzonitrile) and Charge Separation from MP to $^1\text{azaBODIPY}^*$ (in Benzonitrile) of the Porphyrin-azaBODIPY Dyads and Triads

compound	solvent	$k_{\text{ENT}}/\text{s}^{-1}$ ^a	$k_{\text{CS}}/\text{s}^{-1}$ ^b
ZnP-azaBODIPY	toluene	6.6×10^{11}	–
	benzonitrile	6.4×10^{11}	2.9×10^{10}
$(\text{ZnP})_2$ -azaBODIPY	toluene	1.0×10^{12}	–
	benzonitrile	9.6×10^{11}	4.5×10^{10}
H_2P -azaBODIPY	toluene	–	–
	benzonitrile	2.3×10^{11}	6.0×10^9
$(\text{H}_2\text{P})_2$ -azaBODIPY	toluene	–	–
	benzonitrile	4.0×10^{10}	1.6×10^{10}

^aEnergy transfer from $^1\text{MP}^*$ to azaBODIPY. ^bElectron transfer from MP to $^1\text{azaBODIPY}^*$.

both toluene and benzonitrile, the energy-transfer process seems to be efficient for the triads due to the presence of two donor porphyrin entities. Between ZnP and H_2P donors, k_{ENT} values are higher for the ZnP derivatives. The k_{CS} values also seem to follow this trend, that is, they are higher for ZnP as compared to H_2P derived dyads and triads and exhibit improved rates with increase in their numbers.

Supramolecular $\text{C}_{60}\text{py}_2:(\text{ZnP})_2$ -azaBODIPY Tetrad: Formation and Photochemical Studies. The molecular clip-like structure of $(\text{ZnP})_2$ -azaBODIPY prompted us to further use this molecule to build novel supramolecular architecture using fullerene functionalized with two pyridine entities³⁴ suitable for accommodating both the ZnP entities of $(\text{ZnP})_2$ -azaBODIPY, as shown in Figure 1d by a ‘two-point’ axial coordination approach. Figure 8a shows the optical absorption changes during increasing addition of C_{60}py_2 to a solution of $(\text{ZnP})_2$ -azaBODIPY in *o*-dichlorobenzene, a noncoordinating solvent. During the titration, the ZnP bands located at 425 and 550 nm experienced diminished intensity with red shifts of the bands to 432 and 567 nm, respectively, characteristic of axial coordination.³⁵ During the titration, the azaBODIPY band located at 667 nm revealed no spectral shifts, indicating that the added C_{60}py_2 binding to the ZnP entities and not azaBODIPY unit. A Job’s plot mole ratio method was constructed to evaluate the molecular stoichiometry. As shown in Figure 8b, such plots (decrease or increase of Soret band intensity) revealed a break at 1:1 ratio to the added fullerene to the triad, establishing the $\text{C}_{60}\text{py}_2:(\text{ZnP})_2$ -azaBODIPY molecular stoichiometry. The binding constant was evaluated by constructing a Benesi–Hildebrand plot,³⁶ as shown in Figure 8c. Such plot yielded a binding constant K of $1.85 \times 10^5 \text{ M}^{-1}$, which is nearly two orders of magnitude higher than that reported for C_{60}py binding to ZnP³⁵ as a result of two-point binding of the target receptor.

The structure of the supramolecular tetrad $\text{C}_{60}\text{py}_2:(\text{ZnP})_2$ -azaBODIPY was deduced from B3LYP/3-21G(*) studies. As shown in Figure 9, the molecular clip-like structure of the $(\text{ZnP})_2$ -azaBODIPY accommodated the bis-pyridine functionalized fullerene via metal-pyridine axial coordination involving both the ZnP entities. In the optimized structure, the Zn–Zn distance of the two ZnP entities was 12.4 Å, while that of the Zn_1 –B and Zn_2 –B distances between the ZnP and azaBODIPY

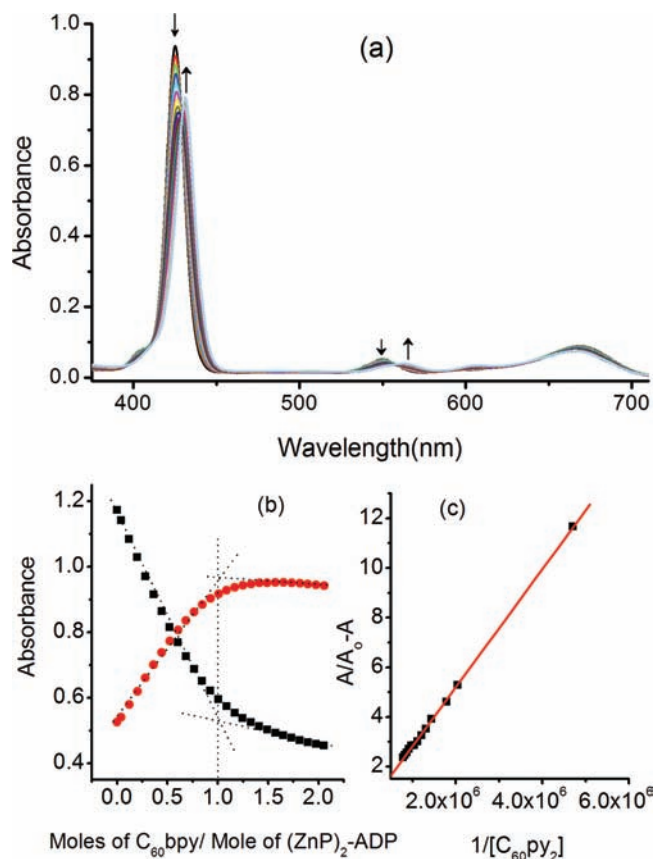


Figure 8. UV–vis spectral changes observed on increasing addition of C_{60}py_2 (0.05 equiv each addition) to $(\text{ZnP})_2$ -azaBODIPY (10 μM) in *o*-dichlorobenzene. (b) Plot of Jobs method of continuous variation for $\text{C}_{60}\text{py}_2:(\text{ZnP})_2$ -azaBODIPY formation monitored at 425 (black) and 432 (red) nm. (c) Benesi–Hildebrand plot where A is the absorbance of the complex formed on increasing addition of C_{60}py_2 and A_0 is the absorbance of the $(\text{ZnP})_2$ -azaBODIPY in the absence of added C_{60}py_2 .

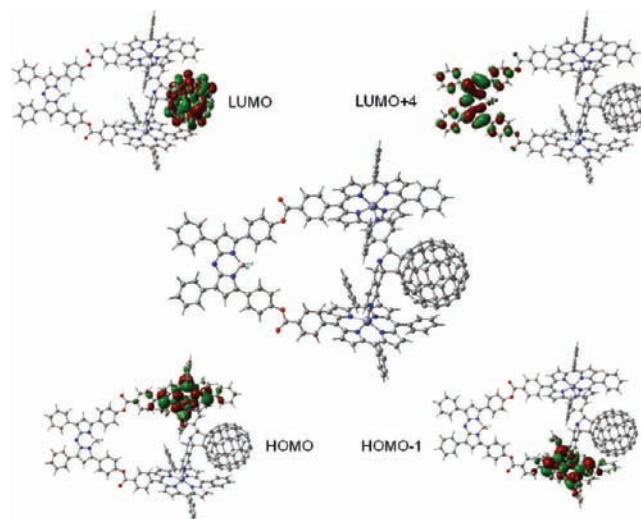


Figure 9. B3LYP/3-21G(*) optimized structure of $\text{C}_{60}\text{py}_2:(\text{ZnP})_2$ -azaBODIPY and the HOMO, HOMO-1, LUMO, and LUMO+4 frontier orbitals.

were 15.7 and 15.4 Å, respectively. Distances between Zn_1 – C_{60} and Zn_2 – C_{60} (center of fullerene) were 5.2 and 5.4 Å, respectively. The B– C_{60} distance was about 16.7 Å. The close proximity of Zn– C_{60} compared to Zn–B was evident from

these studies. The frontier orbitals were also generated to visualize the HOMO and LUMO locations. Both HOMO and HOMO-1 were found to be fully localized on the ZnP entities, while the LUMO was on the fullerene and LUMO+4 was on the azaBODIPY entity of the tetrad.

In order to probe the redox properties of the supramolecular tetrad, $C_{60}py_2:(ZnP)_2$ -azaBODIPY, cyclic voltammetric studies were performed in *o*-dichlorobenzene containing 0.10 M of (*n*-Bu₄N)ClO₄ as a supporting electrolyte, and the results are shown in Figure 10. In contrast to the computational

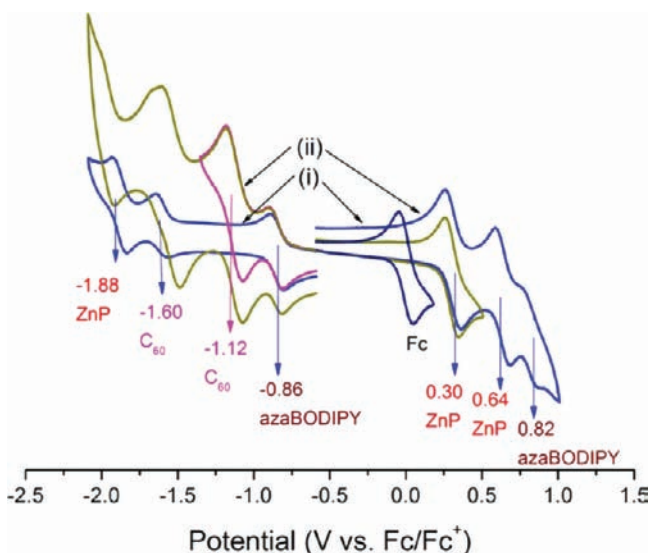


Figure 10. Cyclic voltammograms of (i) $(ZnP)_2$ -azaBODIPY and (ii) $C_{60}py_2:(ZnP)_2$ -azaBODIPY obtained by equimolar addition of $C_{60}py_2$ and $(ZnP)_2$ -azaBODIPY in *o*-dichlorobenzene containing 0.10 M of (*n*-Bu₄N)ClO₄. Scan rate = 100 mV/s. The voltammogram abbreviated as Fc is the one-electron redox wave for the ferrocene internal standard.

expectations, the first cathodic process of the tetrad corresponding to the reduction of azaBODIPY entity was located at -0.86 V, the second and third processes corresponding to the reduction of C_{60} entity were located at -1.12 and -1.60 V vs Fc/Fc^+ , and the fourth reduction potential at -1.88 V corresponds to the reduction of ZnP entity. The discrepancy from the computational results is ascribed to the larger solvation of the radical anion of azaBODIPY as compared to that of the radical anion of C_{60} entity. The anodic waves located at 0.30 V correspond to oxidation of the ZnP entity. The one-electron reduction of azaBODIPY is 250 mV easier as compared to fulleropyrrolidine.

The energetics for PET from $^1ZnP^*$ to azaBODIPY and $^1ZnP^*$ to $C_{60}py_2$ was evaluated using the redox and the earlier discussed spectral data.³³ Such calculations revealed that the charge separation is possible via the both routes ($\Delta G_{CS} = -0.89$ eV and -0.63 eV, respectively), while charge recombination is more exergonic involving fullerene compared to azaBODIPY ($\Delta G_{CR} = -1.16$ eV involving azaBODIPY and -1.42 eV involving $C_{60}py_2$). These results in conjunction with Marcus theory of electron transfer³⁷ suggest electron transfer involving C_{60} and not azaBODIPY. Because an alternative pathway, that is PET from $^1azaBODIPY^*$ to $C_{60}py_2$, reaction is slightly endothermic; such a process is not likely to occur under the present experimental conditions.

As discussed in the previous section, fluorescence studies of $(ZnP)_2$ -azaBODIPY in both toluene and *o*-dichlorobenzene revealed bands at 598 and 650 nm corresponding to ZnP and at 697 nm corresponding to azaBODIPY as a result of energy transfer. Increasing addition of $C_{60}(py)_2$ resulted in a decrease in these emission intensities. This suggests occurrence electron transfer from $^1ZnP^*$ to either azaBODIPY and/or C_{60} (Figure S9, Supporting Information).

In order to unravel the electron-transfer route and obtain the kinetic information, further transient spectral studies at femtosecond time scale were performed, as described below. The $C_{60}(py)_2:(ZnP)_2$ -azaBODIPY was probed with 426 nm excitation to selectively excite the porphyrin fluorophore (Figure 11). The transient absorption spectrum measured at

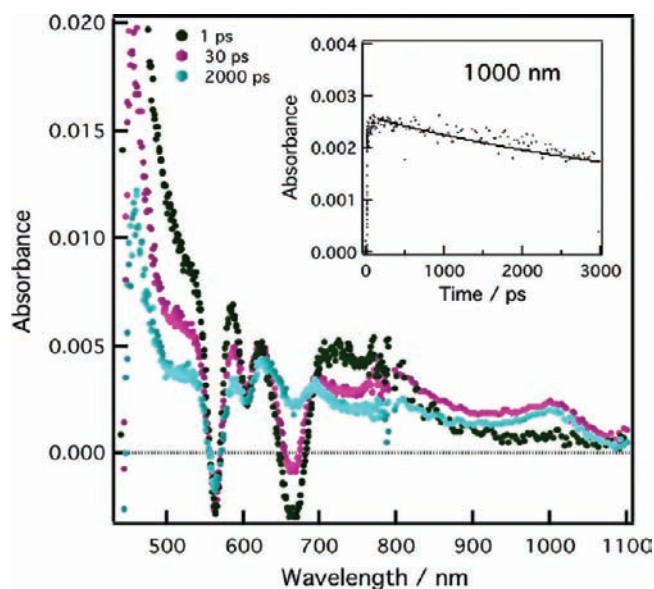


Figure 11. Differential absorption spectra obtained upon femtosecond flash photolysis (420 nm) of the $C_{60}py_2:(ZnP)_2$ -azaBODIPY supramolecular tetrad at the indicated time intervals in toluene. Inset: Rise and decay of the C_{60} radical anion monitored to evaluate the charge-separation and charge-recombination kinetics.

1 ps after femtosecond laser excitation exhibited the transient absorption of the ZnP singlet excited state ($^1ZnP^*$). With time, $^1ZnP^*$ emission peak at 458 nm is diminished in intensity with a concomitant increase in absorbance at 1000 nm due to the formation of $C_{60}^{\bullet-}$ and also absorbance at 620 nm due to $ZnP^{\bullet+}$ formation, providing direct evidence of electron transfer from the photoexcited ZnP unit ($^1ZnP^*$) to the ground state of C_{60} without any indication of energy transfer from $^1ZnP^*$ to azaBODIPY. The kinetics of electron transfer from $^1ZnP^*$ to C_{60} was analyzed by exponential fitting of the rise profile of the $C_{60}^{\bullet-}$ (at 1000 nm) or $ZnP^{\bullet+}$ (at 620 nm) ($k_{CS} = 6.2 \times 10^{10} s^{-1}$ and $k_{CR} = 1.8 \times 10^8 s^{-1}$). Based on the k_{CR} value, the lifetime of the $C_{60}(py)_2^{\bullet-}:(ZnP)_2^{\bullet+}$ -azaBODIPY was determined to be 5.5 ns, which is significantly longer as compared to the reported porphyrin-fullerene supramolecular dyads.⁶

Photoelectrochemical Studies. The occurrence of electron transfer in the present supramolecular polyads prompted us to perform photoelectrochemical studies³⁸ to verify their ability to convert light into electricity. For this purpose, the donor-acceptor entities were electrochemically deposited on a nanocrystalline SnO₂-modified FTO surface.³⁹ Figure 12 shows the incident photon-to-current conversion efficiency

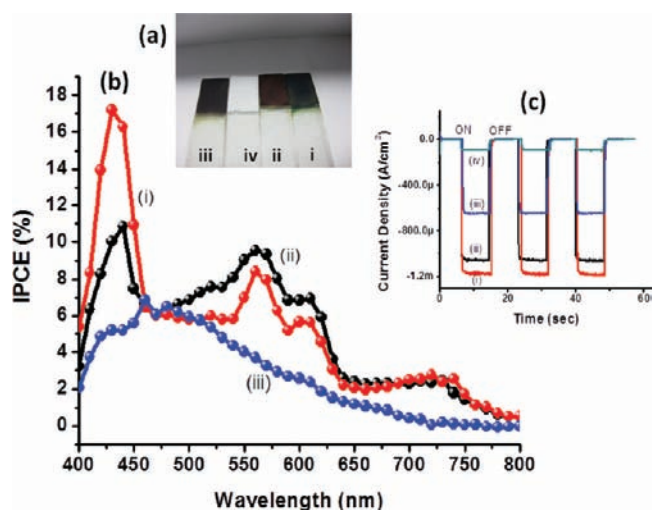


Figure 12. (a) Pictures of FTO/SnO₂ modified electrodes, (b) IPCE(%) curves, and (c) photocurrent on–off switching of (i) C₆₀py₂:(ZnP)₂-azaBODIPY tetrad, (ii) (ZnP)₂-azaBODIPY triad, and (iii) C₆₀py₂:(ZnP)₂ donor–acceptor systems electrophoretically deposited on the surface in acetonitrile solution containing (0.25 M LiI, 0.25 M butyl methyl imidazolium iodide (BMII), 0.05 M I₂) for I^{•−}/I₃[−] redox mediator.

(IPCE%) curves in *o*-dichlorobenzene along with a picture of the modified electrodes and on–off light switching of the photocurrent. The electrophoretic deposition procedure resulted in good coverage of the donor–acceptor entities on the electrode surface (Figure 12a) with optical density of the deposited material close to 1.5. Three modified electrodes, viz., C₆₀py₂:(ZnP)₂, (ZnP)₂-azaBODIPY and C₆₀py₂:(ZnP)₂-azaBODIPY, were used. In the first electrode, C₆₀py₂ was complexed to a covalently linked porphyrin dimer lacking the azaBODIPY entity, (ZnP)₂³⁴, to visualize the importance of azaBODIPY; in the second one, (ZnP)₂-azaBODIPY lacking C₆₀py₂ was employed to visualize the importance of fullerene; and in the third one, the supramolecular tetrad, C₆₀py₂:(ZnP)₂-azaBODIPY, having both fullerene and azaBODIPY were employed. As shown in Figure 12b, the recorded IPCE curves revealed higher currents for the tetrad modified electrode compared to

the other two electrodes lacking either azaBODIPY or fullerene. It is important to note that absorption characteristics of all three entities, viz., ZnP, C₆₀, and azaBODIPY, were clearly seen in the IPCE curve⁴⁰ of the tetrad signifying the importance of the multimodular supramolecular assembly and the involvement of each of the molecular component in higher photocurrent generation. As shown in Figure 12c, photo-switching experiments resulted in consistent currents with a high stability of the deposited material on the electrode surface under the present experimental conditions.

SUMMARY

Control over photoinduced energy and electron transfer in the newly designed and synthesized supramolecular polyads is successfully demonstrated. The energy level diagram shown in Figure 13a, where excitation of MP in the covalently linked MP-azaBODIPY and (MP)₂-azaBODIPY systems, promotes ultrafast efficient energy transfer to generate ¹azaBODIPY* in nonpolar solvent. The ¹azaBODIPY* thus formed deactivates to the ground state directly. Changing the solvent to a more polar benzonitrile changes the deactivation pathway of the energy-transfer product, ¹azaBODIPY* to electron transfer involving MP to generate the charge separation product, (MP)_n^{•+}-azaBODIPY^{•−}. The measured rate constants of *k*_{CS} and *k*_{CR} may be located near the top of Marcus parabola.³⁷

Supramolecular introduction of a second electron acceptor, fullerene, into the molecular assembly promotes electron transfer from the singlet excited MP to the spatially closely located fullerene to generate C₆₀(py)₂^{•−}:(ZnP)₂^{•+}-azaBODIPY charge-separated species in nonpolar solvent, as shown in Figure 13b. That is, control over electron transfer instead of energy transfer has been achieved. Charge stabilization to some extent has also been observed, leading to application of such supramolecular assemblies for direct light energy conversion. Consequently, photoelectrochemical cells were constructed by electrophoretic deposition of different systems on FTO/SnO₂ modified surface. As predicted, higher IPCE(%) values (nearly 17% at the peak maxima) for C₆₀py₂:(ZnP)₂-azaBODIPY modified electrode compared to (ZnP)₂-azaBODIPY modified electrode (~11%) have been observed. The present study successfully demonstrates control over energy and electron

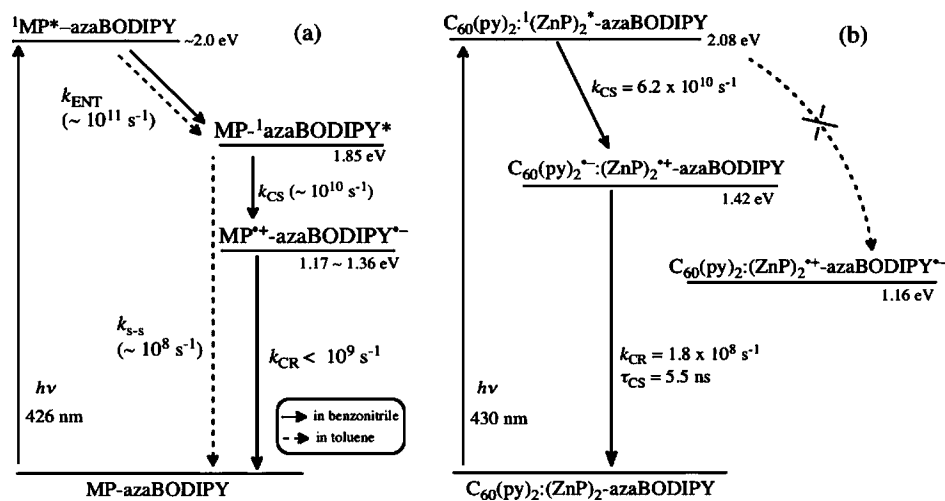


Figure 13. Energy level diagrams showing photochemical events of (a) (MP)_n-azaBODIPY (M = Zn or 2H, *n* = 1, 2) as a function of solvent polarity and (b) C₆₀py₂:(ZnP)₂-azaBODIPY tetrad; both under the conditions of selective excitation of MP.

transfer in molecular polyads and their direct usage in light-energy conversion application.

EXPERIMENTAL SECTION

Chemicals. All the reagents were from Aldrich Chemicals (Milwaukee, WI), while the bulk solvents utilized in the syntheses were from Fischer Chemicals. Tetra-*n*-butylammonium perchlorate, (*n*-Bu₄N)ClO₄, used in electrochemical studies was from Fluka Chemicals. The initial synthesis of ADP macrocycle was performed according to the procedure reported by O'Shea and co-workers²² with necessary modifications.²⁶

The synthetic details of BF₂ chelated [5-(4-hydroxyphenyl)-3-phenyl-1H-pyrrol-2-yl]-[5-(4-hydroxyphenyl)-3-phenylpyrrol-2-ylidene]amine,²⁶ 2-(4'-pyridyl)-5(methylene-4'-pyridyl)-3,4-fulleropyrrolidine (C₆₀(Py)₂),³⁴ 5-(4'-carboxyphenyl)-10,15,20-triphenylporphyrin, and covalently linked zinc porphyrin dimer³⁴ used in photoelectrochemical studies are given elsewhere.

Synthesis of H₂P-azaBODIPY and (H₂P)₂-azaBODIPY. 5-(4'-Carboxyphenyl)-10,15,20-triphenylporphyrin (50 mg, 7.59 × 10⁻⁵ mol) was dissolved in 20 (cm³) of DMF, to which EDCI (14.54 mg, 7.59 × 10⁻⁵ mol) was added at 0 °C under N₂, followed by the addition of BF₂ chelated [5-(4-hydroxyphenyl)-3-phenyl-1H-pyrrol-2-yl]-[5-(4-hydroxyphenyl)-3-phenylpyrrol-2-ylidene]amine (13.39 mg, 2.53 × 10⁻⁵ mol), after which the mixture was stirred for 24 h. Then the solvent was removed under reduced pressure. The residue was dissolved in CH₂Cl₂, and the mixture was washed with water. Then the organic layer was separated and dried over Na₂SO₄, and the solvent was evaporated. The residue was purified by column chromatography on silica gel with CHCl₃:hexanes (1:1) to give (H₂P)₂-azaBODIPY: Yield 5 mg (11%); ¹H NMR (400 MHz, CDCl₃) δ = 8.92–8.8 (m, 16H), 8.63 (d, J = 8.39 Hz, 4H), 8.4 (d, J = 8.41 Hz, 4H), 8.29 (d, J = 8.84 Hz, 4H), 8.25–8.17 (m, 12H), 8.14 (d, J = 6.63 Hz, 4H), 7.8–7.69 (m, 18H), 7.6 (d, J = 8.82 Hz, 4H), 7.56–7.45 (m, 6H), 7.16 (s, 2H), –2.8 (s, 4H) ppm. MALDI-mass: calculated, 1810.8; found, 1812.3. Further elution with CHCl₃ gave compound H₂P-azaBODIPY: Yield 8 mg (27%); ¹H NMR (400 MHz, CDCl₃) δ = 8.91–8.81 (m, 8H), 8.63 (d, J = 8.24 Hz, 2H), 8.41 (d, J = 8.29 Hz, 2H), 8.26–8.19 (m, 8H), 8.14–8.03 (m, 6H), 7.84–7.72 (m, 9H), 7.58–7.44 (m, 8H), 7.12 (s, 1H), 7.08 (s, 1H), 6.99 (d, J = 8.51 Hz, 2H), –2.77 (s, 2H) ppm. MALDI-mass: calculated, 1170.07; found, 1170.98.

Synthesis of ZnP-azaBODIPY. To a H₂P-azaBODIPY (10 mg) dissolved in CHCl₃ (10 cm³), a saturated solution of zinc acetate in methanol (0.1 mL) was added, and the resulting mixture was stirred for 12 h. The mixture was then washed with water, organic layer was separated, dried over anhydrous Na₂SO₄, and rotary evaporated. The residue was purified over silica gel column using CHCl₃:hexanes (4:6) to give compound ZnP-azaBODIPY: Yield 9 mg (85%); ¹H NMR (400 MHz, CDCl₃): δ = 9.01–8.93 (m, 8H), 8.63 (d, J = 8.23 Hz, 2H), 8.41 (d, J = 8.1 Hz, 2H), 8.26–8.19 (m, 8H), 8.14–8.07 (m, 6H), 7.82–7.72 (m, 9H), 7.55–7.43 (m, 8H), 7.12 (s, 1H), 7.08 (s, 1H), 6.99 (d, J = 8.55 Hz, 2H) ppm. MALDI-mass: calculated, 1236.5; found, 1236.21.

Synthesis of (ZnP)₂-azaBODIPY. To a (H₂P)₂-azaBODIPY (10 mg) dissolved in CHCl₃ (10 cm³), saturated solution of zinc acetate in methanol (0.1 mL) was added, and the resulting mixture was stirred for 12 h. The mixture was then washed with water, organic layer was separated, dried over anhydrous Na₂SO₄, and rotary evaporated. The residue was purified over silica gel column using CHCl₃:hexanes (4:6) to give (ZnP)₂-azaBODIPY: Yield 9 mg (84%); ¹H NMR (400 MHz, CDCl₃): δ = 8.99–8.8 (m, 16H), 8.62 (d, J = 8.39 Hz, 4H), 8.39 (d, J = 8.41 Hz, 4H), 8.26–8.18 (m, 16H), 8.15 (d, J = 6.63 Hz, 4H), 7.79–7.67 (m, 18H), 7.6 (d, J = 8.82 Hz, 4H), 7.57–7.43 (m, 6H), 7.16 (s, 1H) ppm. MALDI-mass: calculated, 1937.5; found, 1943.09 (br).

Preparation of Nanocrystalline SnO₂ Electrodes. These were prepared according to the literature procedure⁴¹ with few changes. A 10 mL of SnO₂ colloidal solution (Alfa Aesar, 15%) was dissolved in 10 mL of ethanol, and 500 mL of NH₄OH was added to this solution for stability. About 0.5 mL of colloidal solution was placed on an optically transparent electrode, fluorine-doped indium tin oxide (FTO) (Pilkington TEC-8, 6–9 Λ/square), and dried in air. The

electrodes were annealed in an oven for 1 h in air at 673 K. The estimated thickness of the electrode was around 5–10 μM.⁴²

ASSOCIATED CONTENT

Supporting Information

Additional experimental details, MALDI-mass spectra of the investigated compounds, excitation spectrum of the dyad and triad, transient absorption spectrum of dyad and triad in toluene and benzonitrile, and complete details of ref 31. This material is available free of charge via the Internet at <http://pubs.acs.org>.

AUTHOR INFORMATION

Corresponding Author

Francis.DSouza@UNT.edu; fukuzumi@chem.eng.osaka-u.ac.jp

ACKNOWLEDGMENTS

This work was supported by the National Science Foundation (grant no. 1110942 to FD), a Grant-in-Aid (nos. 20108010 and 21750146), the Global COE (center of excellence) program "Global Education and Research Center for Bio-Environmental Chemistry" of Osaka University from Ministry of Education, Culture, Sports, Science and Technology, Japan, and KOSEF/MEST through WCU project (R31-2008-000-10010-0) from Korea.

REFERENCES

- (1) (a) *The Photosynthetic Reaction Center*; Deisenhofer, J., Norris, J. R., Eds.; Academic Press: New York, 1993. (b) *Molecular Mechanism of Photosynthesis*; Blankenship, R. E., Ed.; Blackwell Science: Oxford, U.K., 2002.
- (2) (a) Gust, D.; Moore, T. A.; Moore, A. L. *Acc. Chem. Res.* **2009**, *42*, 1890–1898. (b) Gust, D.; Moore, T. A. In *The Porphyrin Handbook*; Kadish, K. M., Smith, K. M., Guillard, R., Eds.; Academic Press: San Diego, CA, 2000; Vol. 8, pp 153–190. (c) Wasielewski, M. R. *Acc. Chem. Res.* **2009**, *42*, 1910–1921.
- (3) (a) *Molecular Level Artificial Photosynthetic Materials*; Mayer, G. J., Ed.; Wiley: New York, 1997. (b) Kamat, P. V. *J. Phys. Chem. C* **2007**, *111*, 2834–2860. (c) Umeyama, T.; Imahori, H. *Energy Environ. Sci.* **2008**, *1*, 120–133. (d) Hasobe, T. *Phys. Chem. Chem. Phys.* **2010**, *12*, 44–57. (e) Fukuzumi, S.; Yamada, Y.; Suenobu, T.; Ohkubo, K.; Kotani, H. *Energy Environ. Sci.* **2011**, *4*, 2754–2766.
- (4) (a) de la Torre, G.; Vazquez, P.; Agullo-Lopez, F.; Torres, T. *Chem. Rev.* **2004**, *104*, 3723–3750. (b) Bottari, G.; de la Torre, G.; Guldi, D. M.; Torres, T. *Chem. Rev.* **2010**, *110*, 6768–6816. (c) Guldi, D. M.; Rahman, G. M. A.; Sgobba, V.; Ehli, C. *Chem. Soc. Rev.* **2006**, *35*, 471–487. (d) Fukuzumi, S.; Guldi, D. M. In *Electron Transfer in Chemistry*; Balzani, V., Ed.; Wiley-VCH: New York, 2001; Vol. 2, pp 270–337. (e) Sanchez, L.; Nazario, M.; Guldi, D. M. *Angew. Chem., Int. Ed.* **2005**, *44*, 5374–5382. (f) Delgado, J. L.; Bouit, P.-A.; Filippone, S.; Herranz, M. A.; Martin, N. *Chem. Commun.* **2010**, *46*, 4853–4865.
- (5) (a) Balzani, V.; Bergamini, G.; Ceroni, P. *Coord. Chem. Rev.* **2008**, *252*, 2456–2469. (b) Campbell, W. M.; Burrell, A. K.; Officer, D. L.; Jolley, K. W. *Coord. Chem. Rev.* **2004**, *248*, 1363–1379. (c) Sessler, J. L.; Lawrence, C. M.; Jayawickramarajah, J. *Chem. Soc. Rev.* **2007**, *36*, 314–325.
- (6) (a) D'Souza, F.; Ito, O. *Coord. Chem. Rev.* **2005**, *249*, 1410–1422. (b) D'Souza, F.; Ito, O. *Chem. Commun.* **2009**, 4913–4928. (c) El-Khouly, M. E.; Ito, O.; Smith, P. M.; D'Souza, F. *J. Photochem. Photobiol. C* **2004**, *5*, 79–104. (d) D'Souza, F.; Ito, O. *Chem. Soc. Rev.* **2012**, *41*, 86–96.
- (7) (a) Fukuzumi, S. *Org. Biomol. Chem.* **2003**, *1*, 609–620. (b) Fukuzumi, S. *Phys. Chem. Chem. Phys.* **2008**, *10*, 2283–2297. (c) Fukuzumi, S.; Kojima, T. *J. Mater. Chem.* **2008**, *18*, 1427–1439.

- (d) Fukuzumi, S.; Honda, T.; Ohkubo, K.; Kojima, T. *Dalton Trans.* **2009**, 3880–3889.
- (8) (a) Balzani, V.; Credi, A.; Venturi, M. In *Organic Nanostructures*; Atwood, J. L., Steed, J. W., Eds.; Wiley-VCH: Weinheim, Germany, 2008; pp 1–31. (b) *Energy Harvesting Materials*, Andrews, D. L., Ed.; World Scientific: Singapore, 2005.
- (9) Gust, D.; Moore, T. A.; Moore, A. L. In *From Non-Covalent Assemblies to Molecular Machines*; Sauvage, J.-P., Gaspard, P., Eds.; Wiley-VCH: Weinheim, Germany, 2011; pp 321–354.
- (10) (a) Kroto, H. W.; Heath, J. R.; O'Brien, S. C.; Curl, R. F.; Smalley, R. E. *Nature* **1985**, *318*, 162–163. (b) Smalley, R. E. *Angew. Chem., Int. Ed.* **1997**, *36*, 1595–1601. (c) Xie, Q.; Perez-Cordero, E.; Echegoyen, L. *J. Am. Chem. Soc.* **1992**, *114*, 3978–3980.
- (11) (a) Fukuzumi, S.; Nakanishi, I.; Suenobu, T.; Kadish, K. M. *J. Am. Chem. Soc.* **1999**, *121*, 3468–3474. (b) Imahori, H.; Tkachenko, N. V.; Vehmanen, V.; Tamaki, K.; Lemmetyinen, H.; Sakata, Y.; Fukuzumi, S. *J. Phys. Chem. A* **2001**, *105*, 1750–1756. (c) Ohkubo, K.; Imahori, H.; Shao, J.; Ou, Z.; Kadish, K. M.; Chen, Y.; Zheng, G.; Pandey, R. K.; Fujitsuka, M.; Ito, O.; Fukuzumi, S. *J. Phys. Chem. A* **2002**, *106*, 10991–10998. (d) Fukuzumi, S.; Ohkubo, K.; Imahori, H.; Guldi, D. M. *Chem.–Eur. J.* **2003**, *9*, 1585–1593.
- (12) (a) Fukuzumi, S.; Imahori, H.; Yamada, H.; El-Khouly, M. E.; Fujitsuka, M.; Ito, O.; Guldi, D. M. *J. Am. Chem. Soc.* **2001**, *123*, 2571–2575. (b) Imahori, H.; Tamaki, K.; Guldi, D. M.; Luo, C.; Fujitsuka, M.; Ito, O.; Sakata, Y.; Fukuzumi, S. *J. Am. Chem. Soc.* **2001**, *123*, 2607–2617. (c) Imahori, H.; Guldi, D. M.; Tamaki, K.; Yoshida, Y.; Luo, C.; Sakata, Y.; Fukuzumi, S. *J. Am. Chem. Soc.* **2001**, *123*, 6617–6628.
- (13) (a) David, C.; Ohkubo, K.; Reimers, J. R.; Fukuzumi, S.; Crossley, M. J. *Phys. Chem. Chem. Phys.* **2007**, *9*, 5260–5266. (b) Lee, S. H.; Larsen, A. G.; Ohkubo, K.; Reimers, J. R.; Fukuzumi, S.; Crossley, M. J. *Chem. Sci.* **2011**, *2*, in press. DOI:10.1039/c1sc00614b.
- (14) (a) Garg, V.; Kodis, G.; Chachivilis, M.; Hambourger, M.; Moore, A. L.; Moore, T. A.; Gust, D. *J. Am. Chem. Soc.* **2011**, *133*, 2944–2954. (b) Terazono, Y.; Kodis, G.; Liddell, P. A.; Garg, V.; Moore, T. A.; Moore, A. L.; Gust, D. *J. Phys. Chem. B* **2009**, *113*, 7147–7155. (c) Kodis, G.; Terazono, Y.; Liddell, P. A.; Andreasson, J.; Garg, V.; Hambourger, M.; Moore, T. A.; Moore, A. L.; Gust, D. *J. Am. Chem. Soc.* **2006**, *128*, 1818–1827.
- (15) (a) Sánchez, L.; Sierra, M.; Martin, N.; Myles, A. J.; Dale, T. J.; Rebek, J. Jr.; Wolfgang, S.; Guldi, D. M. *Angew. Chem., Int. Ed.* **2006**, *45*, 4637–4641. (b) Gayathri, S. S.; Wielopolski, M.; Pérez, E. M.; Fernández, G.; Sánchez, L.; Viruela, R.; Orti, E.; Guldi, D. M.; Martin, N. *Angew. Chem., Int. Ed.* **2009**, *48*, 815–819. (c) D'Souza, F.; Maligaspe, E.; Ohkubo, K.; Zandler, M. E.; Subbaiyan, N. K.; Fukuzumi, S. *J. Am. Chem. Soc.* **2009**, *131*, 8787–8797. (d) D'Souza, F.; Subbaiyan, N. K.; Xie, Y.; Hill, J. P.; Ariga, K.; Ohkubo, K.; Fukuzumi, S. *J. Am. Chem. Soc.* **2009**, *131*, 16138–16146. (e) Hill, J. P.; El-Khouly, M. E.; Charvet, R.; Subbaiyan, N. K.; Ariga, K.; Fukuzumi, S.; D'Souza, F. *Chem. Commun.* **2010**, *46*, 7933–7935.
- (16) (a) El-Khouly, M. E.; Ju, D. K.; Kay, K.-Y.; D'Souza, F.; Fukuzumi, S. *Chem.–Eur. J.* **2010**, *16*, 6193–6202. (b) Tanaka, M.; Ohkubo, K.; Gros, C. P.; Guillard, R.; Fukuzumi, S. *J. Am. Chem. Soc.* **2006**, *128*, 14625–14633. (c) Nobukuni, H.; Shimazaki, Y.; Uno, H.; Naruta, Y.; Ohkubo, K.; Kojima, T.; Fukuzumi, S.; Seki, S.; Sakai, H.; Hasobe, T.; Tani, F. *Chem.–Eur. J.* **2010**, *16*, 11611–11623.
- (17) (a) Fukuzumi, S.; Saito, K.; Kashiwagi, Y.; Crossley, M. J.; Gadde, S.; D'Souza, F.; Araki, Y.; Ito, O. *Chem. Commun.* **2011**, *47*, 7980–7982. (b) Fukuzumi, S.; Saito, K.; Ohkubo, K.; Troiani, V.; Qiu, H.; Gadde, S.; D'Souza, F.; Solladié, N. *Phys. Chem. Chem. Phys.* **2011**, *13*, 17019–17022.
- (18) (a) Sessler, J. L.; Karnas, E.; Kim, S. K.; Ou, Z.; Zhang, M.; Kadish, K. M.; Ohkubo, K.; Fukuzumi, S. *J. Am. Chem. Soc.* **2008**, *130*, 15256–15257. (b) Fukuzumi, S.; Ohkubo, K.; Kawashima, Y.; Kim, D. S.; Park, J. S.; Jana, A.; Lynch, V. M.; Kim, D.; Sessler, J. L. *J. Am. Chem. Soc.* **2011**, *133*, 15938–15941.
- (19) (a) Kojima, T.; Honda, T.; Ohkubo, K.; Shiro, M.; Kusukawa, T.; Fukuda, T.; Kobayashi, N.; Fukuzumi, S. *Angew. Chem., Int. Ed.* **2008**, *47*, 6712–6716. (b) Takai, A.; Chkounda, M.; Eggenspieler, A.; Gros, C. P.; Lachkar, M.; Barbe, J.-M.; Fukuzumi, S. *J. Am. Chem. Soc.* **2010**, *132*, 4477–4489. (c) Honda, T.; Nakanishi, T.; Ohkubo, K.; Kojima, T.; Fukuzumi, S. *J. Am. Chem. Soc.* **2010**, *132*, 10155–10163. (d) Takai, A.; Gros, C. P.; Barbe, J.-M.; Fukuzumi, S. *Phys. Chem. Chem. Phys.* **2010**, *12*, 12160–12168.
- (20) Imahori, H.; Sekiguchi, Y.; Kashiwagi, Y.; Sato, T.; Araki, Y.; Ito, O.; Yamada, H.; Fukuzumi, S. *Chem.–Eur. J.* **2004**, *10*, 3184–3196.
- (21) (a) Treibs, A.; Kreuzer, F. H. *Liebigs Ann. Chem.* **1968**, *718*, 208–223. (b) Haugland, R. P. *Handbook of Fluorescent Probes and Research Chemicals*, 6th ed; Molecular Probes: Eugene, OR, 1996.
- (22) (a) Gorman, A.; Killoran, J.; O'Shea, C.; Kenna, T.; Gallagher, W. M.; O'Shea, D. F. *J. Am. Chem. Soc.* **2004**, *126*, 10619–10631. (b) Hall, M. J.; McDonnell, S. O.; Killoran, J.; O'Shea, D. F. *J. Org. Chem.* **2005**, *70*, 5571–5578.
- (23) (a) Loudet, A.; Burgess, K. *Chem. Rev.* **2007**, *107*, 4891–4932. (b) Li, F.; Yang, S. I.; Ciringh, T.; Seth, J.; Martin, C. H. III; Singh, D. L.; Kim, D.; Birge, R. R.; Bocian, D. F.; Holtz, D.; Lindsey, J. S. *J. Am. Chem. Soc.* **1998**, *120*, 10001–10017. (c) Tasiar, M.; O'Shea, D. F. *Bioconjugate Chem.* **2010**, *21*, 1130–1133.
- (24) (a) Palma, A.; Tasiar, M.; Frimannsson, D. O.; Vu, T. T.; Meallet-Renault, R.; O'Shea, D. F. *Org. Lett.* **2009**, *11*, 3638–3641. (b) Murtagh, J.; Frimannsson, D. O.; O'Shea, D. F. *Org. Lett.* **2009**, *11*, 5386–5389.
- (25) (a) McDonnell, S. O.; Hall, M. J.; Allen, L. T.; Byrne, A.; Gallagher, W. M.; O'Shea, D. F. *J. Am. Chem. Soc.* **2005**, *127*, 16360–16361. (b) Flavin, K.; Lawrence, K.; Bartelmess, J.; Tasiar, M.; Navio, C.; Bittencourt, C.; O'Shea, D. F.; Guldi, D. M.; Giordani, S. *ACS Nano* **2011**, *5*, 1198–1206.
- (26) Amin, A. N.; El-Khouly, M. E.; Subbaiyan, N. K.; Zandler, M. E.; Supur, M.; Fukuzumi, S.; D'Souza, F. *J. Phys. Chem. A* **2011**, *115*, 9810–9819.
- (27) El-Khouly, M. E.; Amin, A. N.; Zandler, M. E.; Fukuzumi, S.; D'Souza, F. *Chem.–Eur. J.* in revision, **2011**.
- (28) Amin, A. N.; El-Khouly, M. E.; Subbaiyan, N. K.; Zandler, M. E.; Fukuzumi, S.; D'Souza, F. *Chem. Commun.* **2012**, *48*, 206–208.
- (29) *Principles of Fluorescence Spectroscopy*; Lakowicz, J. R., Ed.; Springer: Singapore, 2006.
- (30) *Modern Molecular Photochemistry*; Turro, N. J., Ed.; University Science Books: Sausalito, CA, 1991.
- (31) *Gaussian 03*; Gaussian, Inc.: Pittsburgh, PA, 2003. For complete details see Supporting Information.
- (32) For a general review on DFT applications of porphyrin-fullerene systems see: Zandler, M. E.; D'Souza, F. C. R. *Chemie* **2006**, *9*, 960–981.
- (33) Rehm, D.; Weller, A. *Isr. J. Chem.* **1970**, *8*, 259–271.
- (34) D'Souza, F.; Gadde, S.; Zandler, M. E.; Itou, M.; Araki, Y.; Ito, O. *Chem. Commun.* **2004**, 2276–2277.
- (35) (a) D'Souza, F.; Deviprasad, G. R.; Rahman, M. S.; Choi, J.-P. *Inorg. Chem.* **1999**, *38*, 2157–2160. (b) D'Souza, F.; Deviprasad, G. R.; Zandler, M. E.; Hoang, V. T.; Klykov, A.; Perera, M.; van Stipdonk, M. J.; El-Khouly, M. E.; Fujitsuka, M.; Ito, O. *J. Phys. Chem. A* **2002**, *106*, 3243–3252.
- (36) Benesi, H. A.; Hildebrand, J. H. *J. Am. Chem. Soc.* **1949**, *71*, 2703–2707.
- (37) (a) Marcus, R. A.; Sutin, N. *Biochim. Biophys. Acta* **1985**, *811*, 265–322. (b) Marcus, R. A. *Angew. Chem., Int. Ed.* **1993**, *32*, 1111–1121.
- (38) Yum, J.-H.; Chen, P.; Grätzel, M.; Nazeeruddin, M. K. *ChemSusChem* **2008**, *1*, 699–707.
- (39) (a) Kutner, W.; Pieta, P.; Nowakowski, R.; Sobczak, J. W.; Kaszkur, Z.; McCarty, A. L.; D'Souza, F. *Chem. Mater.* **2005**, *17*, 5635–5645. (b) Barazzouk, S.; Hotchandani, S.; Kamat, P. V. *Adv. Mater.* **2001**, *13*, 1614–1618.
- (40) The monochromatic incident photon-to-current conversion efficiency (IPCE), defined as the number of electrons generated by light in the outer circuit divided by the number of incident photons, was determined according to the following equation: $IPCE(\%) = 100 \times 1240 \times I_{SC}(\text{mA cm}^{-2}) / [\lambda(\text{nm}) \times P_{in}(\text{mW cm}^{-2})]$, where I_{SC} is the

short-circuit photocurrent generated by the incident monochromatic light and λ is the wavelength of this light with intensity P_{in} .

(41) Bedja, I.; Hotchandani, S.; Kamat, P. V. *J. Phys. Chem.* **1994**, *98*, 4133–4139.

(42) Subbaiyan, N. K.; Maligaspe, E.; D'Souza, F. *ACS Appl. Mater. Interfaces* **2011**, *3*, 2368–2376.